AUTHOR QUERY FORM

Dear Author,

Please check your proof carefully and mark all corrections at the appropriate place in the proof (e.g., by using on-screen annotation in the PDF file) or compile them in a separate list.

For correction or revision of any artwork, please consult http://www.elsevier.com/artworkinstructions.

Any queries or remarks that have arisen during the processing of your manuscript are listed below and highlighted by flags in the proof. Click on the Q link to go to the location in the proof.

Location in article	Query / Remark: **click on the Q link to go** **Please insert your reply or correction at the corresponding line in the proof**
Q1	Please check whether the designated corresponding author is correct, and amend if necessary.
Q2	The spelling of the author name(s) in the text has been changed to "Grandhi and Wolons" to match the reference list. Please check the spelling, and correct if necessary.

Thank you for your assistance.
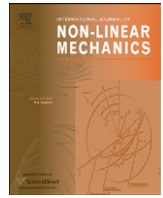
Performance evaluation of shape-memory-alloy superelastic behavior to control a stay cable in cable-stayed bridges

Q1 O. Ben Mekki [a],*, F. Auricchio [b]

[a] University of Tunis EL Manar, ENIT, Laboratory of Civil Engineering (LGC), Tunisia
[b] Department of Structural Mechanics, University of Pavia, Pavia, Italy

ARTICLE INFO

ABSTRACT

This paper focuses on introducing and investigating the performance of a new passive control device for stay cable in cable-stayed bridges made with shape-memory alloys (SMA). The superelasticity and damping capability of SMA is sought in this study to develop a supplementary energy dissipation device for stay cable. A linear model of a sag cable and a one-dimensional constitutive model for the SMA are used. The problem of the optimal design of the device is studied. In the optimization problem, an energy criterion associated with the concept of optimal performance of the hysteretic connection is used. The maximum dissipation energy depends on the cross-sectional area, the length, and the location of the SMA on the cable. The effectiveness of the SMA damper in controlling the cable displacement is assessed. Furthermore, a study is conducted to determine the sensitivity of the cable response to the properties of the SMA device. The comparison between the SMA damper and a more classical passive control energy dissipation device, i.e., the tuned mass damper (TMD), is carried out. The numerical results show the effectiveness of the SMA damper to damp the high free vibration and the harmonic vibration better than an optimal TMD.

© 2010 Elsevier Ltd. All rights reserved.

1. Introduction

Over the last few decades, cable-stayed bridges have attracted great interest because of their aesthetics, structural efficiency, and economy. This type of construction has become popular worldwide in recent years, largely due to the rapid progress in design methodology and construction technologies [26]. However, stay cables are critical structural components in these bridges. Owing to their large flexibility, relatively small mass and extremely low damping, stay cables have frequently exhibited large-amplitude vibrations under wind, wind–rain and support motion. Aerodynamic instability of stay cables with extremely large oscillation amplitude under specific rain and wind conditions has been observed in a number of cable-stayed bridges worldwide, and it is a conundrum to civil engineers [29,39]. Therefore, the mitigation of dynamic response quantities induced by environmental loads is of vital importance in terms of safety and serviceability [2,25].

In the past decade, cable vibration control techniques by means of passive countermeasures, including aerodynamic, mechanical and structural means, have been broadly investigated and successfully implemented [17]. In the meantime, researchers have also studied the active vibration control of cables by applying transverse force control and axial stiffness or tension (support motion) control [30,35].

A lot of researches have been conducted to investigate possible damping systems and to determine the optimal size of viscous dampers attached to cables for vibration control. Kovacs [15] was among the first to investigate the maximum attainable damping ratio for a taut cable with a viscous damper. Pachero et al. [3] proposed a "universal estimation curve" of normalized modal damping ratios versus normalized damper coefficient for a horizontal taut string model. This "universal estimation curve" is generalized by Cremona [5] for inclined cables by taking account of the sag-extensibility parameter. A transfer matrix formulation is developed by Xu et al. [40] to estimate the modal damping ratio of inclined cables attached with oil dampers. Main et al. [18] proposed an analytical formulation of a taut cable with an attached damper. Theoretical studies were also carried out to evaluate the increased damping level of a stay cable after installing passive viscous dampers [2]. It was found that there exists an optimum viscous coefficient of the damper by which the modal damping ratio of a stay cable can reach its maximum for a given mode of vibration. However, this passive device suffers from several drawbacks such as the modal damping ratio of the stay cable decreases rapidly when the viscous coefficient deviates from its optimal value. The use of a variable-orifice viscous damper and electrorheological or magnetorheological (ER/MR) fluid damper with semi-active control may be an alternative [38]. However, the semi-active control device is more complicated to implement. Another

* Corresponding author.
  E-mail address: mekki07@unipv.it (O. Ben Mekki).

candidate that has a great potential for vibration control of stay cable subjected to wind and wind/rain loads is a superelastic shape-memory alloy (SMA) damper with the advantages of large damping capacity, self-centering ability, high fatigue-resistant performance and good corrosion resistance [21].

As a natural consequence of the microscopic behavior, at the macroscopic level shape-memory solids present the superelastic effect (the recovery of large deformations in loading–unloading cycles, occurring at sufficiently high temperatures) and the shape-memory effect (the recovery of large deformations by a combination of mechanical and thermal processes).

These unique properties enable SMA to be used as actuators, passive energy dissipators and dampers for civil structural control [14,1,11,32,31]. When integrated with civil structures, SMAs can be passive, semi-active, or active components to reduce damage caused by environmental impacts.

Using SMAs for passive structure control relies on the SMA's damping capacity, which represents its ability to dissipate vibration energy of structures subject to dynamic loading.

Several authors investigated the energy dissipation of widely used Nitinol superelastic SMA wires. Dolce and Cardone [23] studied superelastic Nitinol wires subjected to tension loading. They observed the dependence of the damping capacity on temperature, loading frequency and the number of loading cycles. **Q2** Grandhi and Wolons [10] proposed using a complex modulus approach to characterize the damping capacity of superelastic SMA wires for convenient integration with structure dynamics. A super-elastic SMA wire demonstrates the damping capacity not only under tension loading, but also under cyclic bending [20]. The numerical results showed that the energy dissipated by the superelastic SMA wire is highly sensitive to its diameter, i.e., the thicker the SMA wire, more energy is dissipated.

SMA energy dissipation devices have been seen in the forms of braces for framed structures [37], connection elements for columns [16], retrofitting devices for historic building [24] and dampers for simply supported bridges [28].

Recently, as large cross-sectional area SMA elements are becoming available, and studies on the properties of SMA bars have attracted more attentions [23,36]. As indicated in Ref. [36], the damping capacity of a martensite Nitinol bar under tension–compression cycles increases with increasing strain amplitude, but decreases with loading cycles and then reaches a stable minimum value. The optimization of the cross-sectional area and the length of the SMA device is presented in [22]. The dynamic performance of the device is evaluated by the steady-state response at the resonance point in order to focus on the damping effect. Analytical formulation utilizing the equivalent linearization approach successfully leads to the basic correlation between the hysteresis shape and the damping effect.

To explore the potentials of SMA based energy dissipation in passive structure control, this paper presents an approach to study the damping vibration of stay cables in a cable-stayed bridge by using a SMA energy dissipation devices with superelastic hysteresis. The first part of the paper presents the general three-dimensional equations of a stay cable subjected to external dynamic loading and controlled by a distribution of dampers in the transverse direction, detailing the hypothesis of the problem linearization. The second part of the paper focuses on three aspects: formulating a mathematical model of the cable with one SMA damper using a Galerkin approximation, verifying the feasibility of the SMA to control the stay cable, and optimizing the SMA device using numerical method. For this simulation a one-dimensional model for superelastic SMA [9] is considered. Finally, the third part of the paper, focuses on the comparison between the TMD and the SMA energy dissipation device to control the stay cable free and harmonic transverse vibration.

2. Dynamic equations formulation of a sag stay cable

A cable is a spatially distributed system, whose transversal dimensions are significantly smaller than longitudinal one. Stay cables have very low levels of inherent mechanical damping and the mechanisms associated with the observed large-amplitude vibrations are still not fully understood. This section has two goals; the first goal is to present the general three-dimensional equations off a stay cable subjected to external dynamic loading and controlled by a distribution of dampers in the transverse direction. The second goal is to introduce the hypothesis leading to the problem linearization; i.e., the assumption of a small sag and the uncoupling of the in-plane and out-of-plane behaviors.

We start considering a cable connecting two points denoted as A and B and placed to a distance L. The segment connecting A and B defines an angle θ versus horizontal axis. For the case of only body load, the cable configuration is planar and we indicate with Axy an orthogonal reference system defined within such a plane. The planar oscillations can occur in the transverse direction (y-axis) as shown in Fig. 1 and non-planar oscillations can occur in direction Az, so that $Axyz$ forms a direct orthogonal frame.

The equations governing the static equilibrium of an inclined cable element subjected only to dead load (gravity) are

$$\begin{cases} \dfrac{\partial}{\partial s}\left[T\dfrac{dx}{ds} \right] = mg\sin\theta \\[2mm] \dfrac{\partial}{\partial s}\left[T\dfrac{dy}{ds} \right] = -mg\cos\theta \end{cases} \tag{1}$$

where s is the Lagrangian co-ordinate, T is the static cable tension, m is the mass of the cable per unit length, and g is the acceleration due to gravity.

A non-linear dynamic model of an inclined cable is built in the coordinate system ($Axyz$) by three coupled partial differential equations [13]:

$$\begin{cases} \dfrac{\partial}{\partial s}\left[(T+\tau)\left(\dfrac{dx}{ds}+\dfrac{\partial u}{\partial s}\right) \right] + F_x(x,t) = m\dfrac{\partial^2 u}{\partial t^2} + mg\sin\theta \\[3mm] \dfrac{\partial}{\partial s}\left[(T+\tau)\left(\dfrac{dy}{ds}+\dfrac{\partial v}{\partial s}\right) \right] + F_y(x,t) - \displaystyle\sum_{i=1}^{M} f_{c,i}(t)\delta(s-s_{c,i}) = m\dfrac{\partial^2 v}{\partial t^2} - mg\cos\theta \\[3mm] \dfrac{\partial}{\partial s}\left[(T+\tau)\dfrac{\partial w}{\partial s} \right] + F_z(x,t) = m\dfrac{\partial^2 w}{\partial t^2} \end{cases} \tag{2}$$

where τ is the dynamic cable tension; u, v and w are the cable dynamic displacement components in the x-, y- and z-directions, respectively, measured from the position of the static equilibrium
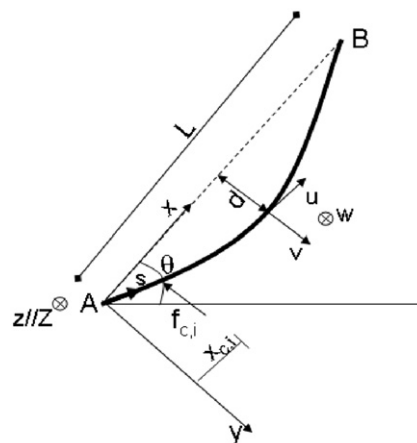

Fig. 1. Schematic diagram of an inclined stay cable.

of the cable; F_x, F_y and F_z are distributed external dynamic loading per unit length in the x-, y- and z-directions, respectively; $f_{c, i}$ are concentrated external force applied by the ith external damper on the cable at the location $s_{c, i}$ in the transverse direction; $s_{c, i}$ is the Lagrangian co-ordinate of the ith dampers measured from the left support of the cable; t is the time; M is the total number of the dampers; $\delta(\cdot)$ is the dirac's delta function.

We consider the following boundary conditions for the cable:

$$\begin{cases} u(0,t) = v(0,t) = w(0,t) = 0 \\ u(L,t) = v(L,t) = w(L,t) = 0 \end{cases} \qquad (3)$$

2.1. Equation of motion for a small sag cable

In a cable-stayed bridge, the stay cables are generally strongly pre-constrained. Thus, the sag is assumed to be small, $ds \approx dx$, and the static tension in the cable is assumed to be constant along the span. Due to these two hypotheses, the static shape of an "inclined cable" is then close to the chord. Accordingly, it is reasonable to approximate this deformation by a parabola whose equation is defined in the local coordinate system (Axyz) as follows [4]:

$$y(x) = 4d \left[\frac{x}{L} - \left(\frac{x}{L} \right)^2 \right] \qquad (4)$$

where $d = mgL^2 \cos\theta / 8T$ is the sag at mid-span.

Using Eqs. (1) governing the static equilibrium and introducing the hypothesis of a small sag cable, system (2) is simplified:

$$\begin{cases} \frac{\partial}{\partial x} \left[(T+\tau)\frac{\partial u}{\partial x} + \tau \right] + F_x(x,t) = m\frac{\partial^2 u}{\partial t^2} \\ \frac{\partial}{\partial x} \left[(T+\tau)\frac{\partial v}{\partial x} + \tau\frac{dy}{dx} \right] + F_y(x,t) - \sum_{i=1}^{M} f_{c,i}(t)\delta(x-x_{c,i}) = m\frac{\partial^2 v}{\partial t^2} \\ \frac{\partial}{\partial x} \left[(T+\tau)\frac{\partial w}{\partial x} \right] + F_z(x,t) = m\frac{\partial^2 w}{\partial t^2} \end{cases} \qquad (5)$$

Finally, it is assumed that the dynamic tension of the cable is related to the non-linear dynamic strain by the following relation [4]:

$$\tau(x,t) = EA\varepsilon(x,t) \qquad (6)$$

where E is Young's modulus, A is the constant cross-sectional area of the cable, and $\varepsilon(x,t)$ is the non-linear axial strain in the cable defined as follows [6]:

$$\varepsilon(x,t) \approx \varepsilon(t) = \frac{\partial u}{\partial x} + \frac{dy}{dx}\frac{\partial v}{\partial x} + \frac{1}{2}\left[\left(\frac{\partial u}{\partial x}\right)^2 + \left(\frac{\partial v}{\partial x}\right)^2 + \left(\frac{\partial w}{\partial x}\right)^2 \right] \qquad (7)$$

2.2. Non-coupled model of small sag stay cable

For a small sag, the cable behaves as a chord; its transversal frequency is smaller than its longitudinal frequency. Therefore, the longitudinal inertia force $m\partial^2 u/\partial t^2$ is assumed to be negligible, and the longitudinal deformation to be small [6]. When considering the longitudinal external forces to be zero, the first equation of system (5) shows that the dynamic tension in the cable can be assumed constant along the cable span. Thus, introducing this result in the two other Eqs. (5), we get

$$\begin{cases} \frac{\partial \tau(x,t)}{\partial x} = 0 \\ (T+\tau)\frac{\partial^2 v}{\partial x^2} + \tau\frac{d^2 y}{dx^2} + F_y(x,t) - \sum_{i=1}^{M} f_{c,i}(t)\delta(x-x_{c,i}) = m\frac{\partial^2 v}{\partial t^2} \\ (T+\tau)\frac{\partial^2 w}{\partial x^2} + F_z = m\frac{\partial^2 w}{\partial t^2} \end{cases} \qquad (8)$$

In order to linearize the previous equations of the small sag cable, the following hypothesis are assumed: small deformations which

implies that second order terms can be neglected, and the dynamic tension is negligible compared to be the static tension. Therefore, the dynamic cable tension can be defined by

$$\tau(t) = EA\left(\frac{\partial u}{\partial x} + \frac{dy}{dx}\frac{\partial v}{\partial x} \right), \qquad (9)$$

and the last two equations of system (8) are written as

$$\begin{cases} T\frac{\partial^2 v}{\partial x^2} + \tau\frac{d^2 y}{dx^2} + F_y(x,t) - \sum_{i=1}^{M} f_{c,i}(t)\delta(x-x_{c,i}) = m\frac{\partial^2 v}{\partial t^2} \\ T\frac{\partial^2 w}{\partial x^2} = m\frac{\partial^2 w}{\partial t^2} \end{cases} \qquad (10)$$

The linear theory applied to a cable with a small sag shows that in-plane and out-of-plane behaviors are essentially uncoupled because this motion involves no additional cable tension (to the first order); the out-of-plane modes and the in-plane antisymmetric modes are the same as those of a taut string, while the in-plane symmetric modes are controlled by the Irvine coefficient.

Using Eq. (9), the longitudinal displacement is deducted from the first equation of system (8), i.e.:

$$\frac{\partial^2 u}{\partial x^2} = -\frac{\partial}{\partial x}\left(\frac{dy}{dx}\frac{\partial v}{\partial x} \right) \qquad (11)$$

By double-integrating equation (11) and introducing the boundary conditions as indicated by system (3), the dynamic tension is given by

$$\tau(t) = -\frac{EA}{L}\frac{d^2 y}{dx^2} \int_0^L v(x,t) \, dx \qquad (12)$$

By replacing Eq. (12) in the first equation of system (10), the transversal displacement of the stay cable verifies this linear equation:

$$m\frac{\partial^2 v}{\partial t^2} - T\frac{\partial^2 v}{\partial x^2} + \frac{EA}{L}\left(\frac{d^2 y}{dx^2} \right)^2 \int_0^L v(x,t) \, dx = F_y(x,t) - \sum_{i=1}^{M} f_{c,i}(t)\delta(x-x_{c,i}) \qquad (13)$$

where $d^2 y/dx^2$ and dy/dx can be deducted from Eq. (4).

This linear model is obtained according to two main hypotheses; the sag cable is small and the in-plane and out-of-plane behaviors are essentially uncoupled. This last model is tackled to study the control of the stay cable considering one SMA damper attached near the cable's lower end.

3. Control of stay cable transverse vibration with one SMA damper

In this section, we consider a stay cable suspended between two supports and equipped by a SMA damper installed at a distance x_c from support A as shown in Fig. 2. Generally, the damper location on the stay cable has to be near a support because it is the most practical position. We assume that the SMA damper produces a force f_c in the y-direction. Considering the end-supports of the cable
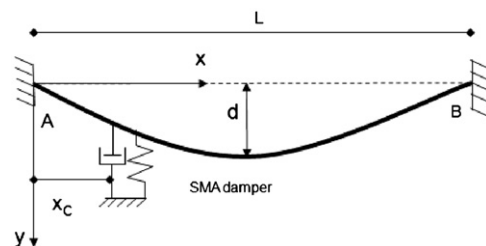

Fig. 2. In-plane stay cable with sag attached with one transverse SMA.

to be fixed, the combined stay cable/SMA system has the following partial differential equation of motion derived from Eq. (13):

$$m\ddot{v} - Tv'' + \frac{EA}{L}(y'')^2 \int_0^L v \, dx = F_y - f_c(t)\delta(x-x_c) \tag{14}$$

where we now use notation, $(')$ and $(\cdot)$ to denote partial derivatives with respect to x and t, respectively, and where we recall that

$$v = v(x,t), \quad F_y = F_y(x,t), \quad \text{and} \quad y = y(x) \tag{15}$$

3.1. Approximate series solutions to equations of motion

The transverse deflexion can be approximated using a finite series

$$v = \sum_{i=1}^{N} \alpha_i(t)\varphi_i(x) \tag{16}$$

where $\alpha_i(t)$ are non-dimensional modal participation factors and $\varphi_i(x)$ are a set of mode shape functions, assumed to be continuous and to satisfy the geometric boundary conditions, i.e., $\varphi_i(0) = \varphi_i(L) = 0$.

To compute the damping and responses of the cable with the SMA damper, we assume sinusoidal shape functions, $\varphi_i(x) = \sin(i\pi x/L)$, identical to the mode shapes of the cable without the damper. Adopting Galerkin approximation based on the free modes of the stay cable, the factors $\alpha_i(t)$ satisfy

$$m_{ii}\ddot{\alpha}_i(t) + (k_{ii} + \lambda^2 m_{ii})\alpha_i(t) = F_{yi} - f_c(t)\varphi_i(x_c) \quad \text{for } i = 1 \ldots N \tag{17}$$

where

$$\begin{cases} \lambda^2 = \frac{EA}{L}\left(\frac{mg\cos\theta}{T}\right)^2 \\ m_{ii} = m\int_0^L \varphi_i(x)\varphi_i(x)\,dx = m\frac{L}{2} \\ k_{ii} = T\int_0^L \varphi'_i(x)\varphi'_i(x)\,dx = \frac{T\pi^2 i^2}{2L} \\ F_{yi} = \int_0^L F_y(x,t)\varphi_i(x)\,dx \\ \varphi_i(x_c) = \sin\left(\frac{i\pi x_c}{L}\right) \end{cases} \tag{18}$$

We observe that the system of dynamical equations (17) are decoupled in all terms except than the term $f_c(t)$ induced by the presence of the SMA damper. So the SMA damper introduces non-linearity into combined linear cable-damper system and Newmark numerical method is used to compute the dynamic response of the cable.

In the following we detail the expression of the damping force $f_c(t)$, which will have a form clearly depending on the SMA constitutive behavior.

3.2. Constitutive model for the SMA system

To reproduce the superelastic behavior of the SMA element introduced in the previous section, we consider the one-dimensional model proposed in Ref. [9]. This model considers one scalar internal variable, ξ_s, representing the martensite fraction, and two processes which may produce martensite fraction variations: the conversion of austenite into martensite $(A \longrightarrow S)$, and the conversion of martensite into austenite $(S \longrightarrow A)$.

Following experimental evidence, both the processes are governed by linear kinetic rules in terms of the uniaxial stress σ. In particular, the activation conditions for the conversion of austenite into martensite are

$$\sigma_s^{AS} < |\sigma| < \sigma_f^{AS} \quad \text{and} \quad \overline{|\dot{\sigma}|} > 0 \tag{19}$$

where σ_s^{AS} and σ_f^{AS} are material parameters, $|\cdot|$ is the absolute value and a superpose dot indicates a time-derivative. The corresponding evolution equation is set equal to

$$\dot{\xi}_s = -(1-\xi_s)\frac{\overline{|\dot{\sigma}|}}{|\sigma| - \sigma_f^{AS}} \tag{20}$$

On the other hand, the activation conditions for the conversion of martensite into austenite are

$$\sigma_f^{SA} < |\sigma| < \sigma_s^{SA} \quad \text{and} \quad \overline{|\dot{\sigma}|} < 0 \tag{21}$$

where σ_f^{SA} and σ_s^{SA} are material parameters. The corresponding evolution equation is set equal to

$$\dot{\xi}_s = \xi_s \frac{\overline{|\dot{\sigma}|}}{|\sigma| - \sigma_f^{SA}} \tag{22}$$

Limiting the discussion to a small deformation regime, the model proposed in Ref. [9] assumes an additive decomposition of the total strain ε:

$$\varepsilon = \varepsilon^e + \varepsilon_L \xi_s \, \text{sgn}(\sigma) \tag{23}$$

where ε^e is the elastic strain, ε_L is the maximum residual strain and $\text{sgn}(\cdot)$ is the sign function. The maximum residual strain ε_L, regarded as a material constant, is a measure of the maximum deformation obtainable only by multiple-variant martensite detwinning, hence, a measure of the maximum deformation obtainable aligning all the single-variant martensites in one direction. Moreover, the presence of $\text{sgn}(\sigma)$ is the later equation indicates that the direction of the effect relative to the martensite fraction ξ_s is governed by the stress. Finally, the elastic strain is assumed to be linearly related to the stress:

$$\sigma = E\varepsilon^e \tag{24}$$

with E the elastic modulus.

The adopted SMA model presents many advantages, such as robustness and simplicity of algorithmic implementation as detailed in Ref. [9].

3.3. Optimization of the cross-sectional area and the length of the SMA wires

In the design of SMA-based damping devices to control a stay cable dynamic, one of the most practical problems to be faced is choosing the appropriate dimensions of SMA elements.

It has been observed that a cable rain/wind-induced response tends to be dominated by the first mode or by the first few modes [34]. For simplicity, in the following analysis, we consider just one vibration mode of the cable. Then the equation of motion of the system is

$$m_{11}\ddot{\alpha}_1(t) + (k_{11} + \lambda^2 m_{11})\alpha_1(t) = F_{y1} - f_c(t)\varphi_1(x_c) \tag{25}$$

In order to give an optimal parameters for the SMA, such as for the cross-sectional area and the length of wires, different criteria may be followed. The most useful criterion design refers to energy-based methods [12]. The idea is that the SMA performs at its best if it is capable of dissipating as much as possible of the total energy of the structure.

The energy balance of the equilibrium equation (25) is defined as follows:

$$E_k(t) + E_e(t) = E_i(t) + E_c(t) \tag{26}$$

where $E_k(t)$ is the stay cable kinetic energy defined as

$$E_k(t) = \frac{1}{2}m_{11}\dot{\alpha}_1^2(t)$$

$E_e(t)$ is the stay cable elastic energy defined as

$$E_e(t) = \frac{1}{2}(k_{11} + \lambda^2 m_{11})\alpha_1^2(t)$$

$E_i(t)$ is the input energy defined as

$$E_i(t) = \int_0^t F_{y1}(t)\dot{\alpha}_1(t)\,dt$$

$E_c(t)$ is the energy associated with the SMA device defined as

$$E_c(t) = E_{ec}(t) + E_{dc}(t)$$

This energy term can be considered as the sum of an elastic term, $E_{ec}(t)$, and of a dissipative term, $E_{dc}(t)$. The dissipative term is the area of hysteresis loop.

The optimal device in free-vibration is chosen when the maximum value of the energy dissipated in the SMA device, $E_{dc}(t)$, is considered. For a fixed position of the SMA, we decided to maximize the force exerted by SMA $f_c(t)$ with the hope that this should load also to augmentation of dissipated energy. The force exerted by SMA has this expression

$$f_c(t) = EA_{SMA}\left(\frac{v(x_c,t)}{L_{SMA}} - \xi_s \varepsilon_L \, \text{sign}(\varepsilon)\right) \qquad (27)$$

where A_{SMA} and L_{SMA} are respectively the cross-sectional area and the length of the SMA device, and $v(x_c,t)$ is the cable transverse displacement at location x_c. For one mode, $v(x_c,t) = \alpha_1(t)\varphi_1(x_c)$.

From Eq. (27), it is clear that to maximize the value of force damper the cross-sectional area of the SMA device should be chosen as big as possible and the length of the SMA device should be chosen as short as passible. Therefore, the appropriate SMA device length should be determined by the following condition:

$$\varepsilon_{SMA}^{max} = \varepsilon_f^{AS} \qquad (28)$$

where ε_f^{AS} is the strain corresponds to the stress finish of the martensite transformation σ_f^{AS} as indicate in Fig. 3. Thus, the optimal length of the SMA device is

$$L_{SMA}^{opt} = \frac{|v^{max}(x_c,t)|}{\varepsilon_f^{AS}} \qquad (29)$$

3.4. Dynamic properties and response of the combined cable-SMA damper system

To investigate the effects of the SMA damper parameters and its location on the damping capability and control efficacy of SMA damper, the stay cable model, which was built and which will be studied in Civil Engineering Laboratory at the University of Tunis, was used to carry out the investigation in this study. The geometric and material properties of the stay cable are listed in Table 1.

The internal damping of the cable is not considered in this work. The stay cable is very flexible structure. However, in this study, the cable is chosen such as its first modal natural frequency, f_1, is equal to 1 Hz. The static tension of this stay cable can be obtained based on the identified first modal natural frequency by using the following expression [13]:

$$T = 4mL^2 f_1^2 = 38.4 \, N \qquad (30)$$

The free-vibration of the stay cable is examined under three different scenarios to determine the effect of the SMA damper cross-sectional area, the effect of the SMA damper length, and finally, the effect of the location of the attached point of the SMA device on the cable. The numerical simulation of the algorithmic model of the SMA is illustrated by Fig. 3 considering this data for the SMA element.

$$\begin{cases} E = 50\,000 \text{ MPa}, & \varepsilon_L = 8\% \\ \sigma_s^{AS} = 500 \text{ MPa}, & \sigma_f^{AS} = 600 \text{ MPa} \\ \sigma_s^{SA} = 250 \text{ MPa}, & \sigma_f^{SA} = 200 \text{ MPa} \end{cases} \qquad (31)$$

3.4.1. Effect of the SMA damper cross-sectional area

To analyse the effect of the SMA cross-sectional area, the non-dimensional modal participation factor for the first mode of the stay cable is plotted by solving Eq. (25) and considering that the SMA damper is located at $x_c/L = 0.1$ and the SMA length is $L_{SMA} = 230$ mm chosen from Eq. (29). Fig. 4 presents the variation of the cable response according to the variation of the SMA cross-sectional area, on the left, and the variation of the SMA force, on the right. Three values of the wire diameter of the SMA damper are chosen. It is clear from this figure that the damping of the stay cable transverse vibration increases while increasing the SMA damper cross-sectional area. This numerical study confirms the analytical conclusion from Eq. (27) concerning the optimization of the SMA wire section.

From this simulation we can observe that the SMA damper is not able to control the small vibration because the SMA deformation is smaller than 1%.

3.4.2. Effect of the length of the SMA damper

In this example, the wire diameter of the SMA damper and the location of the SMA damper are fixed at $D_{SMA} = 0.2$ mm and $x_c/L = 0.1$, respectively, while the length of the SMA is varied as 230, 550, and 750 mm. The steady-state response of the cable versus dimensional time is plotted on the left of Fig. 5, and, on the right, the force SMA damper is plotted versus the displacement of the wire SMA for each L_{SMA}. The damping of the stay cable transverse vibration increases while decreasing the length of the SMA damper. The wire SMA length has more important effect on the small vibrations.

Table 1
Geometric and properties of the stay cable model.

Cable length	L (m)	4.00
Mass per unit length	m (kg m^{-1})	0.6
Inclination angle	θ (deg)	30
Elastic modulus	E (10^{11}N m^2)	0.9

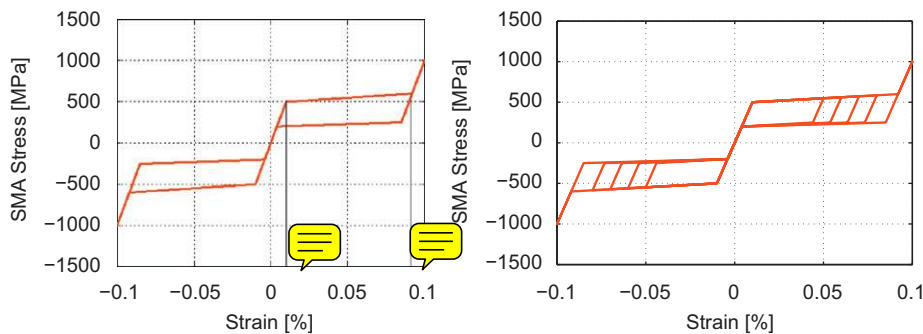**Fig. 3.** Uniaxial test: numerical simulation of the complete tension–compression transformation cycle (left) and numerical simulation of the multiple tension–compression transformation cycles (right).
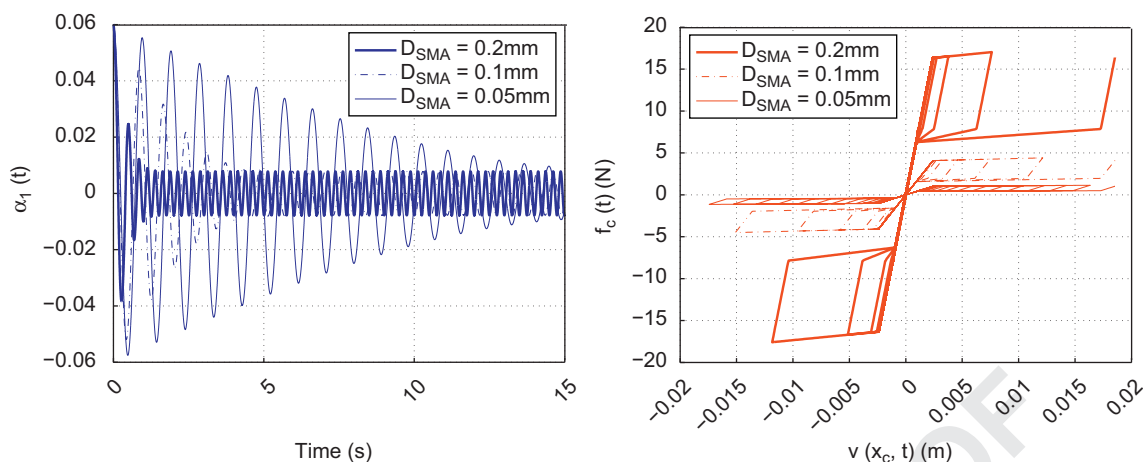
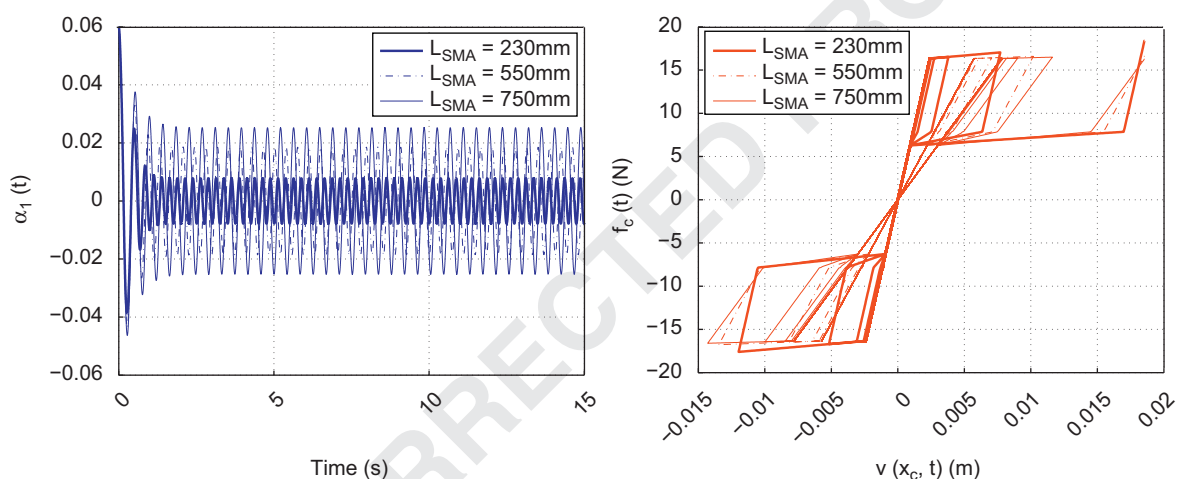**Fig. 4.** Cross-sectional area effect of the SMA damper.

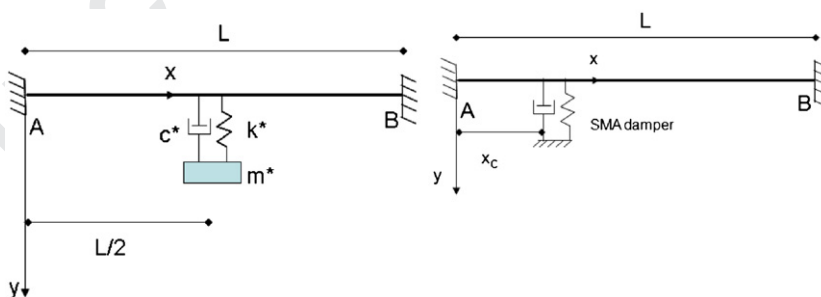**Fig. 5.** Length effect of the SMA damper.

Fig. 6. Combined stay cable with TMD (left) and with SMA damper (right).

4. Comparison between SMA damper and TMD damper to control the stay cable

The real uses of the control systems of the stay cable are the TMD, the cross-ties system, and the MR damper. However, the cross-ties system perturbs the aesthetics of the bridge and the main application of MR is the semi-active control. For this, we choose to compare the SMA with regard to another passive system widely used in practice.

The well known passive control energy dissipation devices in structure control is the tuned mass damper (TMD), which system has been widely used in civil engineering. A large number of buildings, such as Citicorp center, and several bridges, such as Normandie cable-stayed bridge, particularly footbridges such as

Millenium bridge, are now equipped with TMDs [2]. The TMDs are also used to control stay cable in cable-stayed bridges. Tuned mass damper-magnetorheological (TMD-MR) damper for control stay cable is proposed by [8,33]. Analytical, numerical, and experimental studies showed the efficiency of this damper and its practical interest to control stay cable. Ref. [7] used a TMD damper to control the in-plane vibration of two stay cables. The TMD is placed between the twin cables at their midpoints where a significant reduction in vibration levels is notified.

In this section, the idea of the comparison between the optimal TMD and the SMA damper to control the same stay cable that was introduced in the previous section is investigated. The TMD device is considered attached at the midpoint of the cable, optimal

location, as indicated in Fig. 6. In this section, for simplicity, the sag cable is not considered. The equations of the model cable-TMD system are written as follows:

$$\begin{cases} (m_{11}+m^*)\ddot{\alpha}_1(t)+m^*\ddot{y}^*+k_{11}\alpha_1(t)=F_{y1} \\ m^*\ddot{y}^*+m^*\ddot{\alpha}_1(t)+c^*\dot{y}^*+k^*y^*=0. \end{cases} \quad (32)$$

where m^*, k^*, and c^* are the mass, the stiffness and the damping coefficient of the TMD, respectively. y^* is relative displacement of the TMD with respect to cable.

The non-dimensional model of the system can be written as

$$\begin{cases} (1+\mu)\ddot{\alpha}_1+\sqrt{\mu}\ddot{Y}^*+\alpha_1=\dfrac{F_{y1}}{m_{11}\omega_1^2} \\ \ddot{Y}^*+\sqrt{\mu}\ddot{\alpha}_1+2\zeta p\dot{Y}^*+p^2Y^*=0. \end{cases} \quad (33)$$

with

$$\begin{cases} \mu=\dfrac{m^*}{m_{11}}, \quad \omega^*=\sqrt{\dfrac{k^*}{m^*}}, \quad \omega_1=\sqrt{\dfrac{k_{11}}{m_{11}}} \\ \tau=\omega_1 t, \quad \dot{Y}^*=\dfrac{dY^*}{d\tau}, \quad Y^*=\sqrt{\dfrac{1}{\mu}}y^* \\ p=\dfrac{\omega^*}{\omega_1}, \quad \zeta=\dfrac{c^*}{2\,m^*\omega^*} \end{cases} \quad (34)$$

The non-dimensional TMD's parameters μ, p, and ζ are, respectively, related to the dimensional TMD's ones m^*, k^*, and c^*. The optimal parameters of TMD depend on the type of excitation.
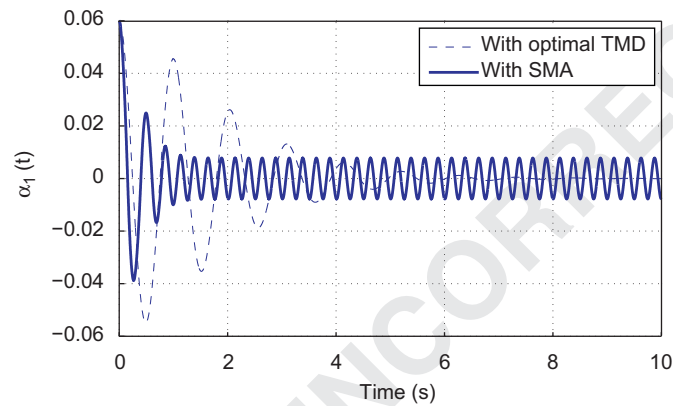

Fig. 7. Comparison between SMA damper and TMD to control the stay cable free vibration.

However, the optimal design of the TMD for a fixed ratio of the TMD mass for free vibration [27] are

$$\begin{cases} p_\mu^{opt}=\dfrac{1}{1+\mu} \\ \zeta_\mu^{opt}=\sqrt{\dfrac{\mu}{1+\mu}} \end{cases} \quad (35)$$

while for an harmonic excitation [19] they are

$$\begin{cases} p_\mu^{opt}=\dfrac{1}{1+\mu} \\ \zeta_\mu^{opt}=\sqrt{\dfrac{3\mu}{8(1+\mu)}} \end{cases} \quad (36)$$

In Fig. 7 the free-response of the stay cable is plotted when it is controlled by TMD and SMA damper, solving, respectively, system (32) and system (25) without external force. The TMD is attached in the midpoint of the cable and these optimal parameters are obtained from system (35) considering $\mu=5\%$. On the other hand, SMA damper is placed near the end with $x_c/L=0.1$. This position is not optimal but it is the most practical position in reality. The length and the cross-sectional area of SMA damper are fixed from the parametric study made in the previous section. These parameters took the optimal values: $L_{SMA}=230$ mm and $D_{SMA}=0.2$ mm.

Fig. 7 shows that the SMA, in its non-optimal position, is able to damp only the high free vibration of the stay cable better than the optimal TMD in its optimal position. However, it is able to damp the harmonic excitation more better than the optimal TMD as shown in Fig. 8. The parameters of the SMA are always the same whereas the optimal parameters of the TMD are obtained in this case according to formula (36).

From Fig. 7, we can observe that the largest vibration response of the SMA dampers controlled cable is around 50% of the one obtained using the TMDs, and the vibration decay speed of the SMA controlled cable is much faster than that of the TMD controlled cable, suggesting that the proposed SMA damper is very effective to reduce structural response. An equivalent viscous damping value of the TMD is 7.3% however the equivalent viscous damping value of the shape-memory alloys is 17.45% when we consider only the vibration response before the stabilization of the oscillation (2 s).

The only one favors of TMD, in free vibration, is able to better damp out the small vibrations.

From the right of Fig. 8 it is observed that without any damping device the cable vibration amplitude is much larger than when the SMA damper is installed.
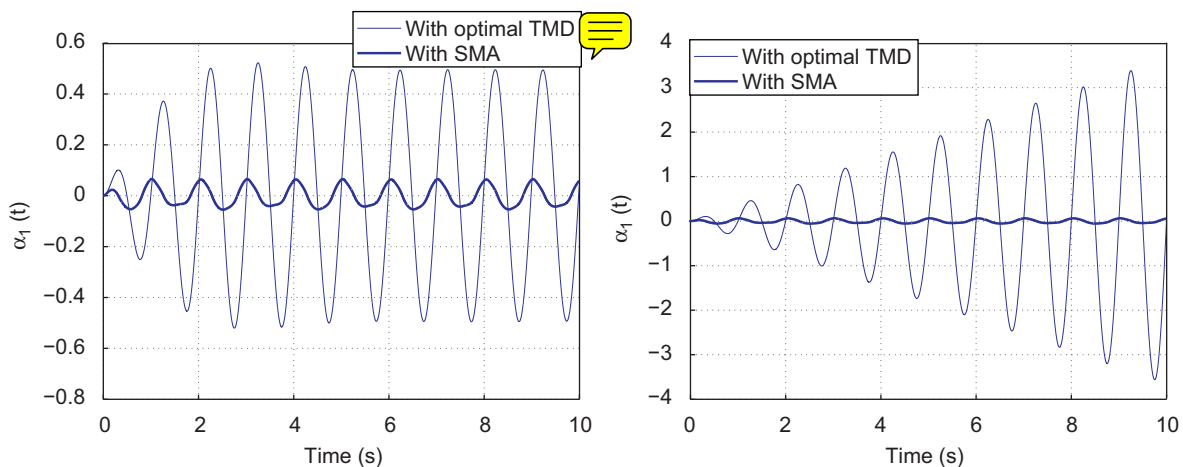

Fig. 8. Comparison between SMA damper and TMD to control the stay cable harmonic vibration (left) and harmonic vibration of the stay cable first mode without actuator and with SMA damper (right).

5. Conclusions

A numerical study on the oscillation mitigation of a combined cable-SMA damper system has been conducted. The purpose of this investigation is to devise a SMA damper with superelastic properties to eliminate most types of oscillations and to understand the optimal parameters such as section and length of the SMA.

The simulation on a cable model with SMA damper showed the excellent property of energy dissipation of the SMA and their ability to suppress the cable vibration. The performance of the SMA damper is notably dependent on the cross-sectional area, the length and the position of the SMA. The cross-sectional area and the length of the SMA device should be chosen, respectively, as big as possible and as short as possible. Finally, the comparison from the SMA damper and the well known passive control energy dissipation devices in structure control, the TMD, showed that the SMA, in its non-optimal position, is able to damp the high free vibration of the stay cable better than the optimal TMD, in its optimal position, and to damp the harmonic excitation more better than the optimal TMD.

References

[1] B. Andrawes, R. DesRoches, Sensitivity of seismic application to different shape memory alloy models, Journal of Engineering Mechanics 183 (2008) 134–173.

[2] B.F. Spenser, S. Nagarajaiah, State of the art of structural control, Journal of Structural Engineering (ASCE) 129 (7) (2003) 845–856.

[3] B.M. Pacheco, Y. Fujino, A. Sulekh, Estimation curve for modal damping in stay cable with viscous damper, Journal of Structural Engineering (ASCE) 119 (9) (1993) 1961–1965.

[4] C. Cremona, Dynamique non linéaire des câbles et application au comportement des ponts haubanés, Revue Française de Mécanique 2 (2000) 107–113.

[5] C. Cremona, A generalisation of the Pacheco's curve for linear damper design. in: Proceedings of the 4th International Symposium on Cable Dynamics, Liege, A.I.M, 2001, pp. 293–308.

[6] C. Cremona, J.C. Foucriat, Comportement au vent des ponts, Presses Ecole Nationale des Ponts et Chaussées (ENPC), 2002.

[7] C.N. Jensen, Optimal damping of stays in cable-stayed bridges for in-plane vibrations, Journal Sound and Vibration 256 (2002) 499–513.

[8] C.S. Cai, M. Asce, W.J. Wu, M. Araujo, Cable vibration control a TMD-MR damper system: experimental exploration, Journal of Structural Engineering (ASCE) 133 (2007) 629–637.

[9] F. Auricchio, E. Sacco, A one-dimensional model for superelastic shape-memory alloys with different elastic properties between austenite and martensite, International Journal of Non-Linear Mechanics 32 (6) (1997) 1101–1114.

[10] F. Grandhi, D. Wolons, Characterization of the pseudoelastic damping behavior of shape memory alloy wires using complex modulus, Smart Materials and Structures 8 (1999) 49–56.

[11] G. Song, N. Ma, H.N. Li, Applications of shape memory alloys in civil structures, Engineering Structures 28 (2006) 1266–1274.

[12] G.W. Housner, L.A. Bergaman, T.K. Caughey, A.G. Chassiakos, R.O. Claus, S.F. Masri, R.E. Skelton, T.T. Soong, B.F. Spencer, J.T.P. Yao, Structural control: past, present, and future, Journal of Engineering Mechanics 123 (9) (1997) 897–971.

[13] H.M. Irvine, Cable Structures, The MIT Press, Cambridge, 1981.

[14] H.N. Li, H. Qian, G.B. Song, D.W. Gao, Type of shape memory alloy damper: design, experiment and numerical simulation, Journal of Vibration Engineering 21 (2008) 179–184.

[15] I. Kovacs, Zur frage der seilschwingungen und der seildampfung, Die Bautechnik 59 (1982) 325–332.

[16] J. Ocel, R. DesRoches, R.T. Leon, J.R. Hayes, S. Sweeney, Steel beam-column connections using shape memory alloys, (ASCE) Journal of Structural Engineering 130 (2004) 731–740.

[17] J.A. Main, S. Jones, Evaluation of viscous dampers for stay-cable vibration mitigation, Journal of Bridge Engineering (ASCE) 6 (6) (2001) 385–388.

[18] J.A. Main, S. Jones, Free vibrations of taut cable with attached damper. Part i: linear viscous damper, Journal of Engineering Mechanics 128 (2002) 1062–1071.

[19] J.P. Den Hartog, Mechanical Vibrations, McGraw Hill Book Co., New York, 1947.

[20] K.H. Ip, Energy dissipation in shape memory alloy wire under cyclic bending, Smart Materials and Structures 9 (2000) 653–659.

[21] L. Hui, L. Min, O. Jinping, Vibration mitigation of stay cable with one shape memory alloy damper, Structural Control and Health Monitoring 11 (2004) 21–36.

[22] M. Arata, N. Mohammad, Optimization of hysteretic characteristics of damping devices based on pseudoelastic shape memory alloys, International Journal of Non-Linear Mechanics 37 (2002) 1375–1386.

[23] M. Dolce, D. Cardone, Mechanical behaviour of shape memory alloys for seismic application 1. Martensite and austenite NiTi bars subjected to torsion, International Journal of Mechanical Sciences 43 (2001) 2631–2651.

[24] M. Indirli, M.G. Castellano, P. Clemente, A. Martelli, Demo application of shape memory alloy devices: the rehabilitation of S. Georgio Church Bell Tower, in: Smart Systems for Bridges, Structures and Highways, SPIE, vol. 4330, 2001, pp. 262–272.

[25] M.D. Symans, M.C. Constantinou, Semi-active control systems for seismic protection of structures: a state-of-the-art review, Engineering Structures 21 (6) (1999) 469–487.

[26] N. Gimsing, Cable-stayed bridges-past, present, and future. in: Proceedings IABSE, 1999.

[27] O. Ben Mekki, F. Bourquin, F. Maceri, C. Nguyen, An adaptive pendulum for evolving structures, in: Proceedings of the 4th IASC World Conference on Structural Control and Monitoring, San Diego, CA, July 2006.

[28] R. DesRoches, M. Delemont, Seismic retrofit of simply supported bridges using shape memory alloys, Engineering Structures 24 (2002) 325–332.

[29] R.W. Poston, Cable-stay conundrum, ASCE Civil Engineering 768 (8) (1998) 58–61.

[30] T. Susumpow, Y. Fujino, Active control of multi-modal cable vibrations by axial support motion, Journal of Engineering Mechanics (ASCE) 121 (1995) 964–972.

[31] V. Torra, A. Isalgue, C. Auguet, F. Martorell, P. Terriault, F.C. Lovey, Built in damping for family homes via SMA: an ANSYS computation scheme based on mesoscopic and microscopic experimental analyses, Engineering Structures 29 (2007) 1889–1902.

[32] V. Torra, A. Isalgue, C. Auguet, G. Carreras, F.C. Lovey, H. Soul, P. Terriault, Damping in civil engineering using SMA. The fatigue behavior and stability of CuAlBe and NiTi alloys, Journal of Materials Engineering and Performance 18 (2009) 738–745.

[33] W.J. Wu, C.S. Cai, Theoretical exploration of a taut cable and a TMD system, Engineering Structures 29 (2007) 962–972.

[34] X.Y. Wang, Y.Q. Ni, J.M. Ko, Z.Q. Chen, Optimal design of viscous dampers for multi-mode vibration control of bridge cables, Engineering Structures 27 (2005) 792–800.

[35] Y. Fujino, P. Warnitchai, B.M. Pacheco, Active stiffness control of cable vibration, Journal of Applied Mechanics (ASME) 60 (1993) 948–953.

[36] Y. Liu, Z. Xie, J.V. Humbeeck, Cyclic deformation of NiTi shape memory alloys, Materials Science and Engineering A 273–275 (1999) 673–678.

[37] Y.L. Han, Q.S. Li, A.Q. Li, A.Y.T. Leung, P.H. Lin, Structural vibration control by shape memory alloy damper, Earthquake Engineering and Structural Dynamics 32 (2003) 483–494.

[38] Y.L. Xu, H.J. Zhou, Damping cable vibration for a cable-stayed bridge using adjustable fluid dampers, Journal of Sound and Vibration 306 (2007) 349–360.

[39] Y.Q. Ni, X.Y. Wang, J.M. Ko, Z.Q. Chen, Field observations of rain–wind-induced cable vibration in cable-stayed Dongting Lake Bridge, Journal of Wind Engineering and Industrial Aerodynamics 95 (2007) 303–328.

[40] Z. Yu, Y.L. Xu, J.M. Ko, A hybrid method for estimating modal damping in sagged cable with damper, Journal of Advances in Structural Engineering 1 (1998) 212–236.